IL NUOVO CIMENTO Vol. 35 C, N. 3 Maggio-Giugno 2012
DOI 10.1393/ncc/i2012-11213-x

Colloquia: TOP2011

ATLAS status

S. Fratina on behalf of the ATLAS Collaboration
University of Pennsylvania - Philadelphia, PA, USA

ricevuto l' 1 Marzo 2012
pubblicato online il 25 Maggio 2012

Summary. — The ATLAS detector is a general-purpose particle detector collecting data at the Large Hadron Collider (LHC) in Geneva, Switzerland. This document reports the ATLAS detector performance during 2011 proton-proton collision data-taking.

PACS 29.90.+r – Other topics in elementary-particle and nuclear physics experimental methods and instrumentation.

1. – Introduction

During 2011 proton-proton run the LHC operated at a centre-of-mass energy of 7 TeV and bunch-spacing of 50 ns. Figure 1(a) shows the development of the maximal instantaneous luminosity throughout the year. Figure 1(b) compares the distribution of the average number of minimum bias interactions per crossing μ before and after the change in the beam squeeze parameter from $\beta^* = 1.5\,\mathrm{m}$ to $\beta^* = 1.0\,\mathrm{m}$ at the end of August 2011. The average μ increased to about 12 after the change. The luminosity-weighted detector uptime was above 97% for all, and above 99% for most of the ATLAS subsystems [1]. The detector recorded 94% of the delivered luminosity corresponding to $5.25\,\mathrm{fb}^{-1}$ [2]. The fraction of operational channels was higher than 96% for all sub-systems, and close to 100% for most. The detector performance is compared to GEANT4 [3] detector simulation [4].

Section **2** describes the ATLAS detector [5] and highlights some of the achievements of 2011 data-taking. Additional information on the reconstructed object identification and performance in ATLAS is given in [6]. Section **3** summarizes the ATLAS trigger system. Finally, sect. **4** reports the result of the luminosity measurement, important for many of the measurements of the ATLAS physics program.

2. – The ATLAS detector

2˙1. *Inner detector*. – The ATLAS Inner Detector (ID) tracking system consists of an innermost silicon-based pixel detector (Pixel), a silicon strip detector (SemiConductor

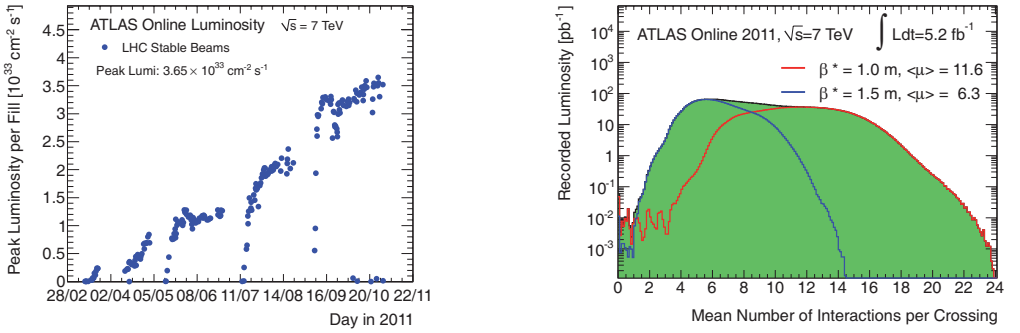

(a) (b)

Fig. 1. – The maximal instantaneous luminosity as a function of day in 2011 (a) and the distribution of the average number of minimum bias interactions per crossing μ (b) [2].

Tracker, SCT) and an outer gaseous drift tube detector with transition radiation measurement capabilities (Transition Radiation Tracker, TRT). The ID is located in a 2 T solenoidal magnetic field and covers a pseudo-rapidity range of $|\eta| < 2.5$ ($|\eta| < 2.0$ for TRT). The design goal for the ID momentum resolution is $\sigma_{p_{\mathrm{T}}}/p_{\mathrm{T}} = 0.05\%\, p_{\mathrm{T}}/\mathrm{GeV} \oplus 1\%$. The measured position resolution is about 10 μm and 25 μm for the precision local x coordinate of the Pixel and SCT, and 120 μm for the TRT [7]. The result is comparable to or exceeding the design resolution of 12 μm and 22 μm for the Pixel and SCT, and 170 μm for the TRT [8]. Excellent silicon position resolution is required for good reconstruction of primary and displaced secondary vertices [9]. The primary vertex z resolution is 100 μm for a vertex with 15 tracks, as shown in fig. 2(a). In addition to its tracking capabilities, the TRT provides discrimination between electrons and pions over the energy range between 1 and 200 GeV by utilizing a transition radiation measurement, as shown fig. 2(b).

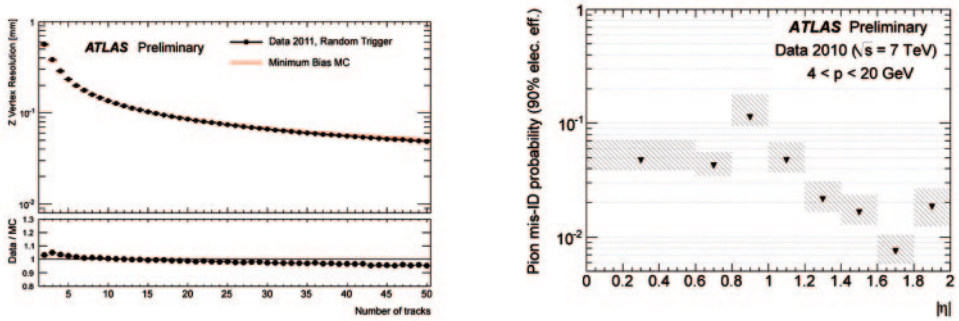

(a) (b)

Fig. 2. – The primary vertex z coordinate resolution as a function of the number of tracks associated to the vertex (a) [10]; and the probability for a pion to pass a transition radiation measurement based electron selection criteria that has 90% efficiency for electrons, as a function of the track pseudo-rapidity η (b) [11].

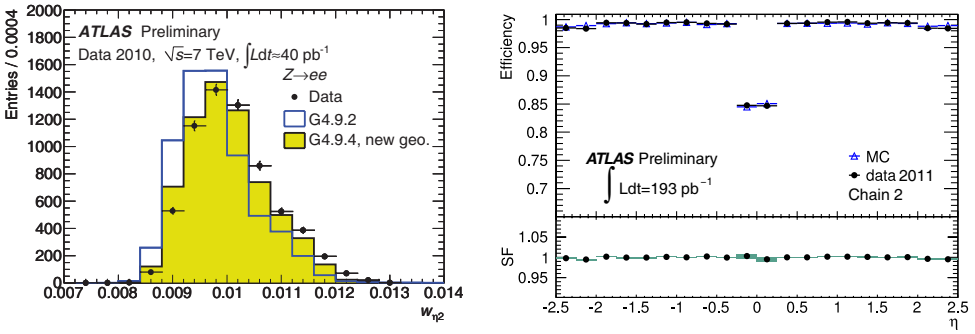

(a) (b)

Fig. 3. – The lateral width of the shower in the middle layer of the electromagnetic calorimeter in data and simulation (a) [12]; and the efficiency for a muon candidate to be successfully reconstructed in the muon spectrometer and associated to an ID track, defined with respect to an ID track (b) [13]. The bottom plot in (b) shows the ratio of measured and predicted efficiency.

2˙2. *The calorimeter system.* – The ID is surrounded by a finely segmented hybrid calorimeter system. An electromagnetic (EM) Pb-LAr (liquid argon) calorimeter, for $|\eta| < 3.2$, is used for electron and photon trigger, identification and energy measurement. Hadronic Fe-scintillator tile calorimeter, for $|\eta| < 1.7$, is used for trigger and jet energy measurements. A hadronic Cu-LAr calorimeter and a forward LAr calorimeter extend the calorimeter coverage up to $|\eta| < 4.9$. A pre-sampler detector installed in front of the EM calorimeter at $|\eta| < 1.8$ is used to correct for the energy loss in the material upstream. The expected EM energy resolution is $\sigma/E \approx 10\%/\sqrt{E/\mathrm{GeV}}$ [5]. Studies of the Z boson mass resolution in $Z \to ee$ events showed the performance in data to be within 10% of that in simulation [12]. A more detailed calorimeter absorber geometry description significantly improved the description of data, as shown in fig. 3(a). The expected high-energy limit for the jet energy resolution is about 3% [5].

2˙3. *The muon spectrometer.* – The muon spectrometer (MS) is the outermost part of the ATLAS detector. Air-core toroidal magnets provide an average magnetic field integral of about 3 Tm. The Monitored Drift Tubes (MDT) arranged in three stations provide precision measurements with about 100 μm position resolution up to $|\eta| < 2.7$. Cathode Strip Chambers are used in place of MDT for the middle of the three stations at $|\eta| > 2.0$. Resistive Plate Chambers in the region up to $|\eta| < 1.05$ and Thin Gap Chambers in the forward region provide the muon trigger and measurement of the non-precision track φ coordinate. The tracks are reconstructed independently in MS and ID, and then combined. Figure 3(b) shows the efficiency for a muon track to be reconstructed in the MS with respect to an ID track. The efficiency is close to 100%, except in the central region where it is smaller due to geometrical acceptance. The p_{T} resolution estimated from the reconstructed $Z \to \mu\mu$ decays is about $\sigma_{p_{\mathrm{T}}}/p_{\mathrm{T}} = 4\%$, and is approaching that of simulation [13].

3. – The trigger system

The events are selected using a three-level trigger system. The hardware-based "Level-1" (L1) system triggers the events at a rate of about 50 kHz, half the design

rate capability. The two high-level triggers (HLT), Level-2 (L2) and Event Filter (EF) are software based, each reducing the event rate by another factor of ten leading to an output rate of about 300 Hz [14]. The L2 trigger decision is based on the measurements in the region of the detector defined by the L1 trigger and the EF selects events based on the measurements in the full detector.

The list of triggers includes a single lepton, di-lepton, di-photon, missing transverse energy $E_{\mathrm{T}}^{\mathrm{miss}}$, multi-jet and combined jet-$E_{\mathrm{T}}^{\mathrm{miss}}$ triggers. In particular, ATLAS maintained a highly efficient single electron (muon) trigger with a low E_{T} (p_{T}) threshold throughout the year. The single electron trigger's efficiency is higher than 95% with respect to an offline reconstructed electron candidate with $E_{\mathrm{T}} > 25\,\mathrm{GeV}$ [15]. An η-dependent threshold at about $E_{\mathrm{T}} = 22\,\mathrm{GeV}$ and a requirement on hadronic core isolation at L1 as well as a transition radiation measurement and a Pixel innermost layer hit requirement at HLT made it possible to maintain single electron triggers with a similar E_{T} threshold also after the luminosity increase in September 2011. The single muon trigger efficiency is about 80% with respect to an offline reconstructed muon with $p_{\mathrm{T}} > 20\,\mathrm{GeV}$, where the main reason for the inefficiency is the geometrical coverage.

4. – The luminosity measurement

The measurement of the recorded integrated luminosity is a crucial ingredient for any cross-section measurement at ATLAS and affects the background estimates in searches for new physics. The ATLAS has two primary luminosity measurement detectors: the LUCID Cherenkov detector at $z = \pm 17\,\mathrm{m}$ and a diamond sensors detector Beam Conditions Monitor (BCM) at $z = \pm 1.8\,\mathrm{m}$ from the interaction point. The BCM was used as a primary luminosity measurement detector in 2011 data-taking. The relation between an observable measured by the BCM and the luminosity was calibrated by performing a dedicated beam separation scan, also known as the van der Meer scan. During this scan, the beam profile is scanned by moving the beams off their nominal positions in two directions and the charge product is measured by dedicated LHC Bunch Current Transformers, which allows an independent measurement of the luminosity. An uncertainty of 3.7% was achieved for data collected until the end of August [16]. The largest single uncertainty affecting the result is a 3.0% uncertainty of the charge product measurement.

5. – Summary

The ATLAS detector collected over $5.25\,\mathrm{fb}^{-1}$ high quality data in 2011. The achieved performance of all detector subsystems is reaching the simulation-based expectations. The analysis of new data has led to improved description of the detector by the simulation and the understanding of the detector performance continues to improve.

REFERENCES

[1] `https://twiki.cern.ch/twiki/bin/view/AtlasPublic/RunStatsPublicResults2010`.
[2] `https://twiki.cern.ch/twiki/bin/view/AtlasPublic/LuminosityPublicResults`.
[3] Agostinelli S. *et al.* (GEANT4 Collaboration), *Nucl. Instrum. Methods A*, **506** (2003) 250.
[4] The ATLAS Collaboration, *Eur. Phys. J. C*, **70** (2010) 823.
[5] The ATLAS Collaboration, *JINST*, **3** (2008) S08003.
[6] Garberson F. on behalf of the ATLAS Collaboration, these proceedings.

[7] The ATLAS Collaboration, ATLAS-CONF-2011-012, http://cdsweb.cern.ch/record/1334582.
[8] The ATLAS Collaboration, ATLAS-TDR-004, http://cdsweb.cern.ch/record/331063.
[9] The ATLAS Collaboration, ATLAS-CONF-2010-069, http://cdsweb.cern.ch/record/1281344.
[10] https://twiki.cern.ch/twiki/bin/view/AtlasPublic/InDetTrackingPerformanceApprovedPlots.
[11] The ATLAS Collaboration, ATLAS-CONF-2011-128, http://cdsweb.cern.ch/record/1383793.
[12] https://twiki.cern.ch/twiki/bin/view/AtlasPublic/ElectronGammaPublicCollisionResults.
[13] https://twiki.cern.ch/twiki/bin/view/AtlasPublic/MuonPerformancePublicPlots.
[14] https://twiki.cern.ch/twiki/bin/view/AtlasPublic/TriggerOperationPublicResults.
[15] https://twiki.cern.ch/twiki/bin/view/AtlasPublic/EgammaTriggerPublicResults.
[16] The ATLAS Collaboration, ATLAS-CONF-2011-116, https://cdsweb.cern.ch/record/1376384.